HHS Public Access

Author manuscript

NMR Biomed. Author manuscript; available in PMC 2022 April 13.

Published in final edited form as:

NMR Biomed. 2018 July ; 31(7): e3930. doi:10.1002/nbm.3930.

Characterizing intra-axonal water diffusion with direction-averaged triple diffusion encoding MRI

Jens H. Jensen[a,b,c,*], **Joseph A. Helpern**[a,b,c,d]

[a]Department of Neuroscience, Medical University of South Carolina, Charleston, South Carolina, USA.

[b]Center for Biomedical Imaging, Medical University of South Carolina, Charleston, South Carolina, USA.

[c]Department of Radiology and Radiological Science, Medical University of South Carolina, Charleston, South Carolina, USA.

[d]Department of Neurology, Medical University of South Carolina, Charleston, South Carolina, USA.

Abstract

For large diffusion weightings, the direction-averaged diffusion MRI (dMRI) signal from white matter is typically dominated by the contribution of water confined to axons. This fact can be exploited to characterize intra-axonal diffusion properties, which may be valuable for interpreting the biophysical meaning of diffusion changes associated with pathology. However, using just the classic Stejskal-Tanner pulse sequence, it has proven challenging to obtain reliable estimates for both the intrinsic intra-axonal diffusivity and the intra-axonal water fraction. Here we propose to apply a modification of the Stejskal-Tanner sequence designed for achieving such estimates. The key feature of the sequence is the addition of a set of extra diffusion encoding gradients that are orthogonal to the direction of the primary gradients, which corresponds to a specific type of triple diffusion encoding (TDE) MRI sequence. Given direction-averaged dMRI data for this TDE sequence, it is shown how the intra-axonal diffusivity and the intra-axonal water fraction can be determined by applying simple, analytic formulae. The method is illustrated with numerical simulations, which suggest it should be accurate for b-values of about 4000 s/mm^2 or higher.

Keywords

intra-axonal; water fraction; pulse sequence; high b-value; direction-averaged; white matter; brain; diffusion MRI

1. INTRODUCTION

Diffusion tensor imaging provides a remarkably practical and reliable means of quantifying several important diffusion properties of biological tissues in vivo, and it is widely applied

*Corresponding Author: Jens H. Jensen, Ph.D., Department of Neuroscience, Medical University of South Carolina, Basic Science Building, MSC 510, 173 Ashley Avenue, Suite 403, Charleston, SC 29425, Tel: (843)876-2467, jense@musc.edu.

for both basic and clinical research, especially to the study of neuropathologies.[1,2] However, the complexity of brain tissue microstructure makes the biophysical interpretation of observed diffusion changes problematic, which has motivated multiple studies aimed at determining diffusion properties of specific cellular compartments such as the intra-axonal space in white matter.[3–12] Despite clear progress in this direction, significant challenges remain, and this continues to be an active area of research.

Recently, it has been shown how to estimate the ratio of the intra-axonal water fraction, f_a, to the square root of the intrinsic intra-axonal diffusivity, D_a, in a simple and direct manner from the direction-averaged diffusion MRI (dMRI) signal, $\bar{S}$.[13] More precisely,

$$\frac{f_a}{\sqrt{D_a}} \approx 2\sqrt{\frac{b}{\pi}} \cdot \frac{\bar{S}}{S_0}, \quad (1)$$

where S_0 is the signal in the absence of diffusion weighting and b is the b-value. The validity of Equation 1 requires that a sufficiently large b-value be used in order to suppress the contribution to the dMRI signal from water in the extra-axonal space, with a minimum b-value of about 4000 s/mm^2 being recommended.[14]

Equation 1 is based on a physical picture in which water inside axons is regarded as being confined to thin cylinders. This idealization has been employed in many prior models of water diffusion in white matter[5,7,9–12,15] and is strongly supported by the observation that the direction-averaged dMRI signal from white matter decreases approximately as $1/\sqrt{b}$ for large diffusion weightings.[14,16] An advantage of using Equation 1, relative to most other approaches for estimating intra-axonal diffusion properties, is that it does not require a particular model for the dMRI signal in brain tissue be numerically fit to experimental data.

A limitation, of course, with Equation 1 is that it provides a rather odd combination of parameters, which may not be the most straightforward to interpret. Having separate estimates for f_a and D_a is certainly preferable, and indeed there are a variety of dMRI signal models for doing just this.[3–6,10–12] However, the predictions of these models are quite variable,[17,18] particularly for the intra-axonal diffusivity, and their calculational prescriptions are substantially more complex than Equation 1.

The main purpose of this paper is to describe an extension of Equation 1 that gives separate values for f_a and D_a in terms of simple analytic functions of direction-averaged dMRI signals. This new approach requires data from a specific triple diffusion encoding (TDE) MRI pulse sequence,[19] which augments the usual Stejskal-Tanner pulse sequence[20] by adding a set of weak diffusion encoding gradients oriented orthogonally to the direction of the main gradients that provide the primary diffusion weighting. This unconventional pulse sequence is not typically available on commercial MRI systems and is inspired by recent work showing the value of dMRI sequences with complex gradient waveforms.[19,21–29] Here we present the theory for this new method, describe numerical simulations that illustrate its application, and discuss practical considerations relevant to the implementation the TDE pulse sequence.

As with Equation 1, our proposed method requires no numerical fitting of signal models to experimental data, but instead gives explicit formulae for f_a and D_a in terms of direction-averaged signal data. The physical picture underlying the formulae is also essentially the same, and a minimum b-value of about 4000 s/mm^2 should again be sufficient to achieve reasonable accuracy. The validation of our proposed method is beyond the scope of this study, but our purpose is to provide a foundation for future work that would implement and test the method for in vivo brain.

2. METHODS

2.1 Triple diffusion encoding (TDE) MRI sequence

For a specified set of diffusion encoding gradients, $\mathbf{G}(t)$, as a function of time t, the components of the b-matrix, $\mathbf{b}$, are given by[30]

$$b_{ij} = \gamma^2 \int_0^T dt \int_0^t dt' \sigma(t') G_i(t') \int_0^t dt'' \sigma(t'') G_j(t''), \tag{2}$$

where G_i is a component of $\mathbf{G}$, $\sigma(t)$ is the spin-flip function, and γ is the proton gyromagnetic ratio. The spin-flip function has a magnitude of one and changes sign at the time of any 180° spin refocusing pulses.[31] Here is it assumed that the gradients play out entirely between $t = 0$ and $t = T$. The essential requirement for the TDE MRI sequence considered here is that the b-matrix has one large eigenvalue, $b_\parallel$, and a pair of degenerate small eigenvalues, which we indicate by $b_\perp$. This means that $\mathbf{b}$ is axially symmetric, with the direction of the symmetry axis, $\mathbf{m}$, being parallel to the eigenvector corresponding to $b_\parallel$. We therefore call $b_\parallel$ the axial b-value and $b_\perp$ the radial b-value. The b-matrix is then completely determined by giving $b_\parallel$, $b_\perp$, and $\mathbf{m}$. For the sake of definiteness, we normalize the symmetry axis direction so that $|\mathbf{m}| = 1$. This terminology and notation for describing axially symmetric b-matrices are also utilized in the prior work of Eriksson and coworkers[22] and is analogous to that often employed for axially symmetric diffusion tensors.[32,33]

For the classic Stejskal-Tanner sequence (Figure 1a), the axial b-value is given by[2,20,30]

$$b_\parallel = (\gamma g \delta)^2 \left(\Delta - \frac{\delta}{3}\right), \tag{3}$$

where g is the magnitude of diffusion encoding gradients, Δ is the diffusion time, and δ is the pulse duration, while the radial b-value is zero.

Our TDE sequence (Figure 1b) maintains the same primary set of diffusion encoding gradients as the Stejskal-Tanner sequence for generating the axial b-value, but adds orthogonal diffusion-encoding gradients to produce the radial b-value. These b-values are then given by

$$b_\parallel = \left(\gamma g_\parallel \delta_\parallel\right)^2 \left(\Delta_\parallel - \frac{\delta_\parallel}{3}\right) \tag{4}$$

and

$$b_\perp = (\gamma g_\perp \delta_\perp)^2 \left(\Delta_\perp - \frac{\delta_\perp}{3}\right), \tag{5}$$

where ($g_\parallel$, $\Delta_\parallel$, $\delta_\parallel$) specifies the gradients for the axial direction and ($g_\perp$, $\Delta_\perp$, $\delta_\perp$) specifies the gradients for the radial direction. Typically, one would choose $g_\parallel \approx g_\perp$, but $\Delta_\parallel > \Delta_\perp$ and $\delta_\parallel \geq \delta_\perp$ so that $b_\parallel > b_\perp$. Since the radial b-value should be much smaller than the axial b-value, the addition of the orthogonal gradients would not necessarily increase the echo time for the sequence by an excessive amount.

2.2 Direction-averaged signal for a single axonal fiber bundle

We model water diffusion inside a single, unidirectional axonal fiber bundle as a Gaussian compartment with an axially symmetric diffusion tensor, $\mathbf{D}_a$. The axial eigenvalue for $\mathbf{D}_a$ is the intrinsic intra-axonal diffusivity, D_a, while the two radial eigenvalues are set to zero. The vanishing of the radial eigenvalues corresponds to the thin cylinder approximation for axons and is justified by the small radii of most axons (~ 1 μm)[34] in comparison to the diffusion length for a typical dMRI experiment (~ 10 μm).[4] We indicate the direction of the symmetry axis for $\mathbf{D}_a$ (i.e., the orientation of the bundle) by the unit vector $\mathbf{n}$.

The contribution of this fiber bundle to the total dMRI signal is then[1,30]

$$S_a(\mathbf{n}, \mathbf{m}) = S_0 F(\mathbf{n}) \exp\left[-\sum_{i,j=1}^{3} b_{ij}(\mathbf{m}) D_{a,ij}(\mathbf{n})\right], \tag{6}$$

where $F(\mathbf{n})$ represents the water fraction for the bundle relative to all dMRI visible water (which normally excludes myelin water due to its short T2) and $D_{a,ij}$ is a component of $\mathbf{D}_a$. We regard the water fraction as a function of $\mathbf{n}$, since bundles oriented in different directions may have different water fractions. Because both the b-matrix and diffusion tensor are axially symmetric, Equation 6 can be simplified to

$$S_a(\mathbf{n}, \mathbf{m}) = S_0 F(\mathbf{n}) \exp\left[-b_\perp D_a - (b_\parallel - b_\perp) D_a (\mathbf{m} \cdot \mathbf{n})^2\right]. \tag{7}$$

By averaging S_a over all directions $\mathbf{m}$ for the b-matrix, one finds

$$\begin{aligned} \bar{S}_a(\mathbf{n}) &\equiv \frac{1}{4\pi} \int d\Omega_{\mathbf{m}} S_a(\mathbf{n}, \mathbf{m}) \\ &= \frac{S_0}{2} F(\mathbf{n}) e^{-b_\perp D_a} \mathrm{erf}\left[\sqrt{(b_\parallel - b_\perp) D_a}\right] \sqrt{\frac{\pi}{(b_\parallel - b_\perp) D_a}}, \end{aligned} \tag{8}$$

where erf indicates the error function. Formulae similar to Equation 8 have been previously derived in Refs. 22 and 23. This type of direction-averaging is also sometimes referred to as taking the spherical mean.[11]

A requirement for our proposed method of estimating f_a and D_a is that $b_\parallel$ is large enough so that $(b_\parallel - b_\perp) D_a \geq 3.4$. When this is true, the error function factor in Equation 8 is equal to one within 1%, and we have the approximation

$$\bar{S}_a(\mathbf{n}) \approx \frac{S_0}{2} F(\mathbf{n}) e^{-b_\perp D_a} \sqrt{\frac{\pi}{(b_\parallel - b_\perp) D_a}}. \quad (9)$$

The simple form of Equation 9 is a key ingredient that enables the derivation of analytic formulae for f_a and D_a in terms of direction-averaged dMRI signals.

2.3 Formulae for intra-axonal diffusivity and intra-axonal water fraction

A particular imaging voxel may, in general, contain an ensemble of fiber bundles oriented in different directions **n**, each with its own water fraction $F(\mathbf{n})$. The contribution to the dMRI signal from all intra-axonal water is then found by integrating Equation 9 over the full ensemble of directions, which yields

$$\bar{S}_{a,tot} \approx \frac{S_0 f_a}{2} e^{-b_\perp D_a} \sqrt{\frac{\pi}{(b_\parallel - b_\perp) D_a}}, \quad (10)$$

where

$$f_a \equiv \int d\Omega_{\mathbf{n}} F(\mathbf{n}) \quad (11)$$

is the intra-axonal water fraction. Here we have taken the intra-axonal diffusivity to be the same for all bundles within a given voxel. Note that diffusion for the full intra-axonal compartment is not necessarily Gaussian, as the combination of two or more Gaussian compartments may have a nonzero kurtosis.[35]

A basic condition for our method is that $b_\perp$ is small. In the special case of $b_\perp = 0$, our TDE sequence reduces to the conventional Stejskal-Tanner sequence and Equation 10 takes the form

$$\bar{S}_{a,tot} \approx \frac{S_0 f_a}{2} \sqrt{\frac{\pi}{b_\parallel D_a}} \quad (12)$$

so that the axonal signal decreases as $1/\sqrt{b_\parallel}$. This square root decay with diffusion weighting is the signature of water confined to thin cylindrical compartments and has been confirmed experimentally.[14,16] An individual Gaussian compartment with a smallest diffusion tensor eigenvalue $\lambda_{\min}$ drops off, in contrast, at least as fast as $\exp(-b_\parallel \lambda_{\min})$, which is a much faster decrease provided $\lambda_{\min} > 1/b_\parallel$. Thus if the diffusion tensor eigenvalues for all extra-axonal water compartments substantially exceed $1/b_\parallel$, then the intra-axonal contribution will dominate the direction-averaged signal. This is the physical picture underlying Equation 1 (see Ref. 13 for a more detailed discussion) and is plausible since one may reasonably expect extra-axonal water to be relatively mobile in all directions.[11] For any $b_\perp << b_\parallel$, this same idealization continues to apply to our direction-averaged TDE signal. The full signal is then approximately equal to $\bar{S}_{a,tot}$, as given by Equation 10, with extra-axonal water giving a negligible contribution for sufficiently strong diffusion weightings.

Now suppose the direction-averaged signal is measured with b-matrices for two different choices of the axial and radial b-values, namely ($b_\parallel$, 0) and ($b_\parallel$, $b_\perp$). The first measurement would then be a conventional Stejskal-Tanner acquisition, as shown in Figure 1a, while the second would include the additional radial diffusion encoding gradients, as depicted in Figure 1b. Let the signal for ($b_\parallel$, 0) be $\bar{S}_1$ and the signal for ($b_\parallel$, $b_\perp$) be $\bar{S}_2$. If Equation 10 is used to approximate these measurements, then one obtains a set of two equations that can be solved for f_a and D_a to find

$$f_a = \frac{2\bar{S}_1}{S_0} \cdot \sqrt{\frac{b_\parallel D_a}{\pi}}, \tag{13}$$

and

$$D_a = \frac{1}{b_\perp} \ln\left(\frac{\bar{S}_1}{\bar{S}_2} \cdot \sqrt{\frac{b_\parallel}{b_\parallel - b_\perp}} \right), \tag{14}$$

which constitute the core formulae for our method of characterizing intra-axonal water diffusion. Note that Equation 13 is equivalent to Equation 1.

2.4 Effect of signal noise

dMRI is an inherently noisy measurement technique, particularly when, as for our proposed method, strong diffusion weightings are utilized. Because dMRI employs magnitude images, the signal noise is not strictly Gaussian, but is still approximately Gaussian if the signal magnitude is at least a few times greater than the rectified noise floor.[36] Here we estimate the effects of signal noise on predictions for f_a and D_a, as obtained with Equations 13 and 14 using, for the sake of simplicity, a Gaussian noise approximation.

By applying a standard error propagation formula[37] to Equations 13 and 14, one finds that the variance for D_a is

$$\delta^2 D_a = \frac{4 b_\parallel D_a}{\pi f_a^2 b_\perp^2} \left[1 + \left(1 - \frac{b_\perp}{b_\parallel} \right) e^{2 b_\perp D_a} \right] \frac{\sigma^2}{N S_0^2}, \tag{15}$$

where σ^2 is the noise variance and N is the number diffusion encoding directions employed. Similarly, the variance for f_a is

$$\delta^2 f_a = f_a^2 \frac{\sigma^2}{N_0 S_0^2} + \frac{b_\parallel}{\pi b_\perp^2 D_a} \left[(2 b_\perp D_a + 1)^2 + \left(1 - \frac{b_\perp}{b_\parallel} \right) e^{2 b_\perp D_a} \right] \frac{\sigma^2}{N S_0^2}, \tag{16}$$

where N_0 is the number independent acquisitions for S_0. For a fixed acquisition time, the variance for f_a is minimized by choosing N_0 so that

$$N_0 \approx N f_a \sqrt{\frac{2\pi b_\perp^2 D_a}{b_\parallel}} \left[(2 b_\perp D_a + 1)^2 + \left(1 - \frac{b_\perp}{b_\parallel} \right) e^{2 b_\perp D_a} \right]^{-1/2}. \tag{17}$$

Because Equations 13 and 14 are nonlinear in the signal, there will also be an estimation bias due to noise.[37] For D_a, the bias is

$$\Delta D_a = \frac{2b_{\|}D_a}{\pi f_a^2 b_{\perp}}\left[\left(1-\frac{b_{\perp}}{b_{\|}}\right)e^{2b_{\perp}D_a}-1\right]\frac{\sigma^2}{NS_0^2}, \tag{18}$$

while for f_a, it is

$$\Delta f_a = f_a\frac{\sigma^2}{N_0S_0^2}+\frac{b_{\|}(2b_{\perp}D_a-1)}{2\pi b_{\perp}^2 D_a f_a}\left[1+\left(1-\frac{b_{\perp}}{b_{\|}}\right)e^{2b_{\perp}D_a}\right]\frac{\sigma^2}{NS_0^2}. \tag{19}$$

A reasonable choice for $b_{\perp}$ may be found by minimizing the variance for D_a of Equation 15. Assuming $b_{\perp} << b_{\|}$, this yields

$$b_{\perp} \approx \frac{1.1}{D_a}. \tag{20}$$

However, this result does not take into account potential gains in SNR that a reduction in $b_{\perp}$ may allow.

As an example, let us consider $N = 128$, $b_{\|} = 4000$ s/mm^2, $b_{\perp} = 500$ s/mm^2, $D_a = 2.2$ μm^2/ms, and $f_a = 0.5$ μm^2/ms. Then Equation 17 gives $N_0 = 14$. From Equations 15 and 16, one finds

$$\delta^2 D_a \approx \frac{12.5}{\mathrm{SNR}^2}\left(\mu\mathrm{m}^2/\mathrm{ms}\right)^2 \tag{21}$$

and

$$\delta^2 f_a \approx \frac{0.35}{\mathrm{SNR}^2}, \tag{22}$$

where SNR ≡ S_0/σ is the signal-to-noise ratio. For the noise bias, Equations 18 and 19 yield

$$\Delta D_a \approx \frac{2.4}{\mathrm{SNR}^2}\quad \mu\mathrm{m}^2/\mathrm{ms} \tag{23}$$

and

$$\Delta f_a \approx \frac{0.23}{\mathrm{SNR}^2}. \tag{24}$$

With an SNR of 50, the expected standard deviation for D_a would then be about $(\delta^2 D_a)^{1/2} = 0.07$ μm^2/ms, while the standard deviation for f_a would be $(\delta^2 f_a)^{1/2} = 0.01$. The corresponding biases are likewise $\Delta D_a = 0.001$ μm^2/ms and $\Delta f_a = 0.0001$.

2.5 Numerical simulations

In order to illustrate the application of Equations 13 and 14, we performed numerical simulations for a model in which the diffusion dynamics of the extra-axonal space is Gaussian and fully characterized by an axially symmetric diffusion tensor with an axial diffusivity of $\lambda_{e,\parallel}$ and a radial diffusivity of $\lambda_{e,\perp}$. The direction-averaged dMRI signal from the extra-axonal water is then

$$\bar{S}_e = \frac{S_0}{2}(1-f_a)e^{-b_\parallel \lambda_{e,\perp} - b_\perp \lambda_{e,\parallel} - b_\perp \lambda_{e,\perp}} \operatorname{erf}\left[\sqrt{(b_\parallel - b_\perp)(\lambda_{e,\parallel} - \lambda_{e,\perp})}\right] \sqrt{\frac{\pi}{(b_\parallel - b_\perp)(\lambda_{e,\parallel} - \lambda_{e,\perp})}}, \quad (25)$$

which is analogous to Equation 8. Similarly, the exact direction-averaged signal for the intra-axonal compartment is obtained by integrating Equation 8 over the all fiber bundle orientations, yielding

$$\bar{S}_{a,tot} = \frac{S_0}{2} f_a e^{-b_\perp D_a} \operatorname{erf}\left[\sqrt{(b_\parallel - b_\perp) D_a}\right] \sqrt{\frac{\pi}{(b_\parallel - b_\perp) D_a}}. \quad (26)$$

The total exact direction-averaged dMRI signal for our model is thus $\bar{S} = \bar{S}_e + \bar{S}_{a,tot}$.

For the simulations, the following parameter choices were employed: $1000 < b_\parallel < 8000$ s/mm^2; $0 < b_\perp < 4000$ s/mm^2; $\lambda_{e,\parallel} = 2.0$ μm^2/ms; $\lambda_{e,\perp} = 1.0$ μm^2/ms; $D_a = 1.0, 1.5, 2.0, 2.5$ μm^2/ms; $f_a = 1/3, 1/2, 2/3$. With these choices, Equations 13 and 14 were used to estimate D_a and f_a, which were compared to the exact values.

3. RESULTS

Numerical results for the estimated D_a values, as obtained from Equation 14, are shown in Figure 2. As $b_\parallel$ is increased with $b_\perp = 500$ s/mm^2, the estimated D_a converges to the exact D_a, with an accuracy of 5% or better being achieved for $b_\parallel$ exceeding 4000 s/mm^2. The convergence to the exact values becomes somewhat more rapid as the intra-axonal water fraction is increased. This is reasonable, since a larger f_a implies a smaller extra-axonal water fraction and hence a smaller extra-axonal contribution to the dMRI signal. With $b_\parallel = 4000$ s/mm^2, the estimated D_a varies by less than 4% for $b_\perp$ values between 0 and 2000 s/mm^2.

Similar numerical results for f_a estimated with Equation 13 are shown in Figure 3. The predicted values with $b_\perp = 500$ s/mm^2 are accurate to better than 7% if $b_\parallel > 4000$ s/mm^2, while with $b_\parallel = 4000$ s/mm^2, they vary as a function of $b_\perp$ by less than 2% as long as $b_\perp < 2000$ s/mm^2. For $b_\parallel = 4000$ s/mm^2 and $b_\perp = 500$ s/mm^2, the error in f_a ranges from 1.4% for $f_a = 2/3$ with $D_a = 1.0$ μm^2/ms to 6.3% for $f_a = 1/3$ with $D_a = 2.5$ μm^2/ms.

4. DISCUSSION

This work has proposed a new method for estimating the intrinsic intra-axonal diffusivity and intra-axonal water fraction in white matter. It is distinguished from most alternative

methods in that D_a and f_a are calculated directly from simple analytic formulae that depend only on direction-averaged dMRI signal data and the chosen b-values, while alternative techniques typically involve nonlinear fitting with detailed models for the dMRI signal.[4,6–12] By circumventing the need for such numerical fitting, errors associated with a sensitive dependence on the model assumptions may be reduced.

A premise underlying the method is that the direction-averaged dMRI signal in white matter is dominated, for large b-values, by the contribution of intra-axonal water. This is supported by recent experiments showing a $1/\sqrt{b}$ decay in the direction-averaged signal as the diffusion weighting is increased, for b-values exceeding about 4000 s/mm^2.[14,16] Prior work has exploited this to estimate the ratio $f_a/\sqrt{D_a}$ by using the formula of Equation 1.[13,14,16,38] Here we have extended this approach to give separate predictions for D_a and f_a.

Another assumption the method relies on is neglecting water exchange between the intra-axonal and extra-axonal compartments, which requires TE to be small in comparison to the inter-compartmental water exchange time. Although not known precisely, the water exchange time in white matter has been estimated as approximately 1 s,[39] which is indeed substantially longer than typical TE values employed with dMRI. We have also idealized the axons as straight cylinders. However, this may not be well justified in some white matter regions, such as the optic nerve, that have undulations with wavelengths of a few tens of microns.[40]

The main innovation of our method is the application of a specific TDE pulse sequence that gives the critical information needed to fix D_a via Equation 14. Once D_a is known, then f_a is easily determined from the ratio $f_a/\sqrt{D_a}$, which is the content of Equation 13. Our TDE sequence is identical to the Stejskal-Tanner sequence, except with additional diffusion encoding gradients that are oriented in directions orthogonal to the primary gradients in a manner so as to make the b-matrix axially symmetric. Similar sequences have been previously applied to characterize microstructure of diffusive media in several prior studies.[22,23,26,29] For gradient strengths of 80 mT/m and a radial b-value of 500 s/mm^2, it would take about 50 ms to play out the full set of radial diffusion encoding gradients. The axial gradients for $b_\parallel$ = 4000 s/mm^2 would also take about 50 ms, implying TE would have to exceed 100 ms after the time for the imaging gradients is included. While this is certainly a significantly longer minimum echo time for our TDE sequence in comparison to a standard Stejskal-Tanner sequence, it is not so long as to preclude implementing this method on state-of-the-art clinical MRI systems. Some reduction in TE is possible by utilizing more complex waveforms (e.g., helical) for the radial diffusion encoding gradients than those depicted in Figure 2, but this is unlikely to yield a large improvement with the relatively small radial b-values considered here. Prior studies using direction-averaged dMRI have employed 64 to 256 diffusion encoding directions,[11–14,38] and we expect a similar number to be appropriate for our proposed method.

To illustrate the application of Equations 13 and 14, we performed a series of numerical simulations. These show how the estimated values for D_a and f_a approach the exact values as the axial b-value, $b_\parallel$, is increased. For our choice of model parameters, we find that fairly good accuracy is achieved for $b_\parallel$ > 4000s/mm^2, which is the same threshold suggested

in a prior related study.[14] However, this could depend somewhat on brain region, due to variability in the diffusion properties of the extra-axonal space. Moreover, prior work suggests that there is a significant T2 difference between the intra-axonal and extra-axonal compartments.[12,41,42] This means that the apparent compartmental water fractions could depend on TE, which may also then affect the accuracy of the D_a and f_a estimates. Compartmental T1 differences are less likely to be important, as long as TR is long in comparison to both the intra-axonal and extra-axonal T1 values.

Our numerical results also suggest that the accuracy of the D_a and f_a estimates are fairly insensitive to the choice of $b_\perp$ provided $b_\perp << b_\parallel$. However, our analysis of the effect of signal noise indicates that the precision of D_a is optimized with $b_\perp \approx 1.1/D_a$ for a fixed SNR.

The most closely related alternative technique to the one described here is by Dhital and coworkers,[29] who also use TDE sequences with high b-values. However, they employ strong radial gradients to suppress the extra-axonal signal with a weak axial gradient to sensitize the signal to D_a, so that the roles of the axial and radial gradients are reversed. In our opinion, method proposed here is appreciably simpler and more comprehensive. This is reflected in the fact that Dhital and coworkers only consider white matter voxels for which the axonal fibers were mainly unidirectional and the intra-axonal water fraction is not estimated. Nonetheless, Dhital and coworkers do present experimental data, finding D_a = 2.25±0.03 μm^2/ms, which supports the feasibility of our closely related reciprocal approach. A similar value for D_a was found in rat spinal cord by Skinner and coworkers using a double diffusion encoding sequence.[27]

In this paper, we have focused on determining D_a and f_a, the two most basic parameters for quantifying intra-axonal water diffusion. However, it would be natural to combine our method with other dMRI approaches to obtain a more comprehensive characterization of water diffusion in white matter. For example, the same data used to determine the direction-averaged dMRI signal for $b_\perp = 0$ (i.e., $\bar{S}_1$) could also be used with fiber ball imaging[13] in order to determine the fiber orientation density function for the axonal bundles. The combination of D_a and the fiber orientation density function is sufficient to then calculate the total diffusion tensor for the intra-axonal space, $\mathbf{D}_{a,tot}$. If the dMRI signal from myelin water is negligible, the diffusion tensor, $\mathbf{D}$, for the full white matter is related to $\mathbf{D}_{a,tot}$ by

$$\mathbf{D} = f_a \mathbf{D}_{a,tot} + (1 - f_a)\mathbf{D}_e, \tag{27}$$

where $\mathbf{D}_e$ is the diffusion tensor for the extra-axonal space. The tensor $\mathbf{D}_e$ is well-defined provided inter-compartmental water exchange time is long in comparison TE, as discussed above. By solving Equation 27 for $\mathbf{D}_e$, one finds

$$\mathbf{D}_e = \frac{\mathbf{D} - f_a \mathbf{D}_{a,tot}}{(1 - f_a)}. \tag{28}$$

Since $\mathbf{D}$ can be measured with diffusion tensor imaging[1,2] and since f_a is known from Equation 13, it is then possible to also construct $\mathbf{D}_e$ in a straightforward manner. In this

way, intra-axonal and extra-axonal diffusion properties can be independently calculated, which can help to elucidate the microstructural origin of diffusion changes associated with neuropathologies such as stroke,[43] epilepsy,[44] and Alzheimer's disease.[45] Note that Equation 28 does not rely on a specific model for diffusion in the extra-axonal compartment.

A limitation of this study is the absence of experimental data, due to the TDE sequence being nonstandard and therefore not readily available on most MRI scanners. Nonetheless, we believe it is important to first describe the theoretical foundation of our approach prior to its implementation, in order to motivate and guide the experimental development. Although the ultimate assessment of our proposed method will require such empirical work, its feasibility is supported by prior research utilizing direction-averaged dMRI, as well as by the numerical simulations presented here.

5. CONCLUSION

The intra-axonal diffusivity and intra-axonal water fraction in white matter may be estimated from direction-averaged dMRI data for strong diffusion weightings by using simple analytic formulae. This provides a more direct and potentially reliable method of determining these diffusion properties than the conventional approach of numerical fitting a full signal model to dMRI data. However, to apply the method, direction-averaged data from the proposed TDE sequence would be required.

ACKNOWLEDGEMENTS

This work was supported, in part, by a grant from the Litwin Foundation (to J. Helpern).

Grant sponsors:

Litwin Foundation

Abbreviations used:

dMRI	diffusion MRI
TDE	triple diffusion encoding

REFERENCES

1. Le Bihan D, Mangin JF, Poupon C, Clark CA, Pappata S, Molko N, Chabriat H. Diffusion tensor imaging: concepts and applications. J Magn Reson Imaging. 2001;13(4):534–546. DOI: 10.1002/jmri.1076. [PubMed: 11276097]
2. Alexander AL, Lee JE, Lazar M, Field AS. Diffusion tensor imaging of the brain. Neurotherapeutics. 2007;4(3):316–329. DOI: 10.1016/j.nurt.2007.0. [PubMed: 17599699]
3. Assaf Y, Freidlin RZ, Rohde GK, Basser PJ. New modeling and experimental framework to characterize hindered and restricted water diffusion in brain white matter. Magn Reson Med. 2004;52(5):965–978. DOI: 10.1002/mrm.20274. [PubMed: 15508168]
4. Jespersen SN, Kroenke CD, Østergaard L, Ackerman JJ, Yablonskiy DA. Modeling dendrite density from magnetic resonance diffusion measurements. Neuroimage. 2007;34(4):1473–1486. DOI: 10.1016/j.neuroimage.2006.10.037. [PubMed: 17188901]

5. Fieremans E, Jensen JH, Helpern JA. White matter characterization with diffusional kurtosis imaging. Neuroimage. 2011;58(1):177–188. DOI: 10.1016/j.neuroimage.2011.06.006. [PubMed: 21699989]

6. Wang Y, Wang Q, Haldar JP, Yeh FC, Xie M, Sun P, Tu TW, Trinkaus K, Klein RS, Cross AH, Song SK. Quantification of increased cellularity during inflammatory demyelination. Brain. 2011;134(Pt12):3590–3601. DOI: 10.1093/brain/awr307. [PubMed: 22171354]

7. Panagiotaki E, Schneider T, Siow B, Hall MG, Lythgoe MF, Alexander DC. Compartment models of the diffusion MR signal in brain white matter: a taxonomy and comparison. Neuroimage. 2012;59(3):2241–2254. DOI: 10.1016/j.neuroimage.2011.09.081. [PubMed: 22001791]

8. Zhang H, Schneider T, Wheeler-Kingshott CA, Alexander DC. NODDI: practical in vivo neurite orientation dispersion and density imaging of the human brain. Neuroimage. 2012;61(4):1000–1016. DOI: 10.1016/j.neuroimage.2012.03.072. [PubMed: 22484410]

9. Ferizi U, Schneider T, Panagiotaki E, Nedjati-Gilani G, Zhang H, Wheeler-Kingshott CA, Alexander DC. A ranking of diffusion MRI compartment models with in vivo human brain data. Magn Reson Med. 2014;72:1785–92. DOI: 10.1002/mrm.25080. [PubMed: 24347370]

10. Hui ES, Russell Glenn G, Helpern JA, Jensen JH. Kurtosis analysis of neural diffusion organization. Neuroimage. 2015;106:391–403. DOI: 10.1016/j.neuroimage.2014.11.015. [PubMed: 25463453]

11. Kaden E, Kelm ND, Carson RP, Does MD, Alexander DC. Multi-compartment microscopic diffusion imaging. Neuroimage. 2016;139:346–359. DOI: 10.1016/j.neuroimage.2016.06.002. [PubMed: 27282476]

12. Veraart J, Novikov DS, Fieremans E. TE dependent Diffusion Imaging (TEdDI) distinguishes between compartmental T2 relaxation times. Neuroimage. 2017; online. DOI: 10.1016/j.neuroimage.2017.09.030.

13. Jensen JH, Glenn GR, Helpern JA. Fiber ball imaging. Neuroimage. 2016;124:824–833. DOI: 10.1016/j.neuroimage.2015.09.049. [PubMed: 26432187]

14. McKinnon ET, Jensen JH, Glenn GR, Helpern JA. Dependence on b-value of the direction-averaged diffusion-weighted imaging signal in brain. Magn Reson Imaging. 2017;36:121–127. DOI: 10.1016/j.mri.2016.10.026. [PubMed: 27989904]

15. Behrens TE, Woolrich MW, Jenkinson M, Johansen-Berg H, Nunes RG, Clare S, Matthews PM, Brady JM, Smith SM. Characterization and propagation of uncertainty in diffusion-weighted MR imaging. Magn Reson Med. 2003;50:1077–1088. DOI: 10.1002/mrm.10609. [PubMed: 14587019]

16. Veraart J, Fieremans E, Novikov DS. Universal power-law scaling of water diffusion in human brain defines what we see with MRI. arXiv preprint; arXiv:1609.09145 [physics.bio-ph]. 2016 Sept 28.

17. Jelescu IO, Veraart J, Fieremans E, Novikov DS. Degeneracy in model parameter estimation for multi-compartmental diffusion in neuronal tissue. NMR Biomed. 2016;29(1):33–47. DOI: 10.1002/nbm.3450. [PubMed: 26615981]

18. Jelescu IO, Veraart J, Adisetiyo V, Milla SS, Novikov DS, Fieremans E. One diffusion acquisition and different white matter models: how does microstructure change in human early development based on WMTI and NODDI? Neuroimage. 2015;107:242–256. DOI: 10.1016/j.neuroimage.2014.12.009. [PubMed: 25498427]

19. Shemesh N, Jespersen SN, Alexander DC, Cohen Y, Drobnjak I, Dyrby TB, Finsterbusch J, Koch MA, Kuder T, Laun F, Lawrenz M. Conventions and nomenclature for double diffusion encoding NMR and MRI. Magn Reson Med. 2016;75:82–87. DOI: 10.1002/mrm.25901. [PubMed: 26418050]

20. Stejskal EO, Tanner JE. Spin diffusion measurements: spin echoes in the presence of a time-dependent field gradient. J Chem Phys. 1965;42(1):288–292. DOI: 10.1063/1.1695690.

21. Shemesh N, Özarslan E, Komlosh ME, Basser PJ, Cohen Y. From single-pulsed field gradient to double-pulsed field gradient MR: gleaning new microstructural information and developing new forms of contrast in MRI. NMR Biomed. 2010;23:757–780. DOI: 10.1002/nbm.1550. [PubMed: 20690130]

22. Eriksson S, Lasič S, Nilsson M, Westin CF, Topgaard D. NMR diffusion-encoding with axial symmetry and variable anisotropy: Distinguishing between prolate and oblate microscopic

diffusion tensors with unknown orientation distribution. J Chem Phys. 2015;142:104201. DOI: 10.1063/1.4913502. [PubMed: 25770532]

23. de Almeida Martins JP, Topgaard D. Two-dimensional correlation of isotropic and directional diffusion using NMR. Phys Rev Lett. 2016;116:087601. DOI: 10.1103/PhysRevLett.116.087601. [PubMed: 26967442]
24. Topgaard D Director orientations in lyotropic liquid crystals: diffusion MRI mapping of the Saupe order tensor. Phys Chem Chem Phys. 2016;18:8545–8553. DOI: 10.1039/C5CP07251D. [PubMed: 26948308]
25. Westin CF, Knutsson H, Pasternak O, Szczepankiewicz F, Özarslan E, van Westen D, Mattisson C, Bogren M, O'donnell LJ, Kubicki M, Topgaard D. Q-space trajectory imaging for multidimensional diffusion MRI of the human brain. Neuroimage. 2016;135:345–362. DOI: 10.1016/j.neuroimage.2016.02.039. [PubMed: 26923372]
26. Topgaard D Multidimensional diffusion MRI. J Magn Reson. 2017;275:98–113. DOI: 10.1016/j.jmr.2016.12.007. [PubMed: 28040623]
27. Skinner NP, Kurpad SN, Schmit BD, Tugan Muftuler L, Budde MD. Rapid in vivo detection of rat spinal cord injury with double-diffusion-encoded magnetic resonance spectroscopy. Magn Reson Med. 2017;77:1639–1649. DOI: 10.1002/mrm.26243. [PubMed: 27080726]
28. Nilsson M, Larsson J, Lundberg D, Szczepankiewicz F, Witzel T, Westin CF, Bryskhe K, Topgaard D. Liquid crystal phantom for validation of microscopic diffusion anisotropy measurements on clinical MRI systems. Magn Reson Med. 2017. DOI: 10.1002/mrm.26814.
29. Dhital B, Reisert M, Kellner E, Kiselev VG. Intra-axonal diffusivity in brain white matter. arXiv preprint; arXiv:1712.04565 [physics.bio-ph]. 2017 Dec 12.
30. Mattiello J, Basser PJ, Le Bihan D. Analytical Expressions for the b matrix in NMR diffusion. J Magn Reson A. 1994;108:131–141. DOI: 10.1006/jmra.1994.1103.
31. Jensen JH, Chandra R. Weak-diffusion theory of NMR signal in magnetically heterogeneous media. J Magn Reson. 1997;126:193–199. DOI: 10.1006/jmre.1997.1178.
32. Anderson AW. Measurement of fiber orientation distributions using high angular resolution diffusion imaging. Magn Reson Med. 2005;54:1194–1206. DOI: 10.1002/mrm.20667. [PubMed: 16161109]
33. Hansen B, Khan AR, Shemesh N, Lund TE, Sangill R, Eskildsen SF, Østergaard L, Jespersen SN. White matter biomarkers from fast protocols using axially symmetric diffusion kurtosis imaging. NMR Biomed. 2017. DOI: 10.1002/nbm.3741.
34. Aboitiz F, Scheibel AB, Fisher RS, Zaidel E. Fiber composition of the human corpus callosum. Brain Res. 1992;598(1–2):143–153. DOI: 10.1016/0006-8993(92)90178-C. [PubMed: 1486477]
35. Jensen JH, Helpern JA. MRI quantification of non-Gaussian water diffusion by kurtosis analysis. NMR Biomed. 2010;23:698–710. DOI: 10.1002/nbm.1518. [PubMed: 20632416]
36. Gudbjartsson H, Patz S. The Rician distribution of noisy MRI data. Magn Reson Med. 1995;34(6):910–914. DOI: 10.1002/mrm.1910340618. [PubMed: 8598820]
37. Ku HH. Notes on the use of propagation of error formulas. J Res Natl Bur Stand. 1966;70C:263–273.
38. Jensen JH, McKinnon ET, Glenn GR, Helpern JA. Evaluating kurtosis-based diffusion MRI tissue models for white matter with fiber ball imaging. NMR Biomed. 2017;30. DOI: 10.1002/nbm.3689.
39. Nilsson M, Lätt J, van Westen D, Brockstedt S, Lasič S, Ståhlberg F, Topgaard D. Noninvasive mapping of water diffusional exchange in the human brain using filter-exchange imaging. Magn Reson Med. 2013;69:1572–1580. DOI: 10.1002/mrm.24395.
40. Nilsson M, Lätt J, Ståhlberg F, Westen D, Hagslätt H. The importance of axonal undulation in diffusion MR measurements: a Monte Carlo simulation study. NMR Biomed. 2012;25:795–805. DOI: 10.1002/nbm.1795. [PubMed: 22020832]
41. Peled S, Cory DG, Raymond SA, Kirschner DA, Jolesz FA. Water diffusion, T2, and compartmentation in frog sciatic nerve. Magn Reson Med. 1999;42:911–918. DOI: 10.1002/(SICI)1522-2594(199911)42:5<911::AID-MRM11>3.0.CO;2-J. [PubMed: 10542350]
42. Dortch RD, Apker GA, Valentine WM, Lai B, Does MD. Compartment-specific enhancement of white matter and nerve ex vivo using chromium. Magn Reson Med. 2010;64:688–697. DOI: 10.1002/mrm.22460. [PubMed: 20806376]

43. Fung SH, Roccatagliata L, Gonzalez RG, Schaefer PW. MR diffusion imaging in ischemic stroke. Neuroimaging Clin N Am. 2011;21(2):345–377. DOI: 10.1016/j.nic.2011.03.001. [PubMed: 21640304]

44. Winston GP. The potential role of novel diffusion imaging techniques in the understanding and treatment of epilepsy. Quant Imaging Med Surg. 2015;5(2):279–287. DOI: 10.3978/j.issn.2223-4292.2015.02.03. [PubMed: 25853085]

45. Amlien IK, Fjell AM. Diffusion tensor imaging of white matter degeneration in Alzheimer's disease and mild cognitive impairment. Neuroscience. 2014;276:206–215. DOI: 10.1016/j.neuroscience.2014.02.017. [PubMed: 24583036]

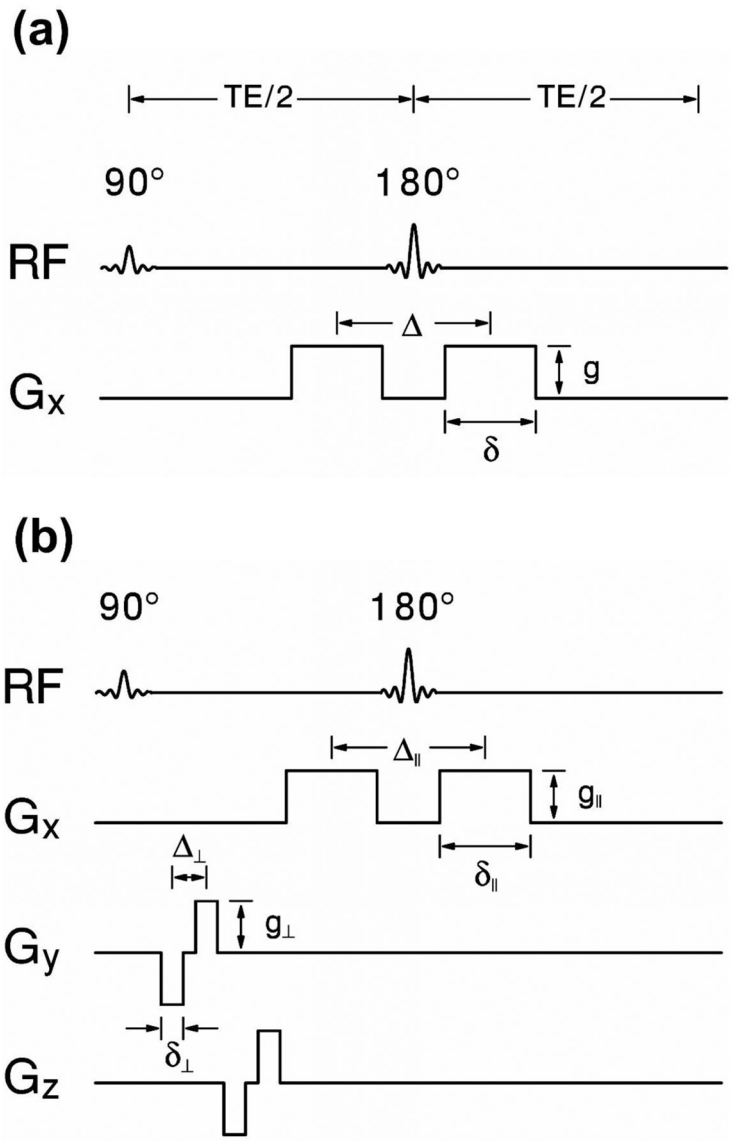

Figure 1:

(a) The classic Stejskal-Tanner sequence[20] with the diffusion encoding gradients oriented in the x-direction. A 180° spin refocusing pulse is placed at TE/2 in order to reduce the deleterious effects of background gradients. The key sequence parameters are the gradient strength g, the diffusion time Δ, and the pulse duration δ. The imaging gradients are not shown, but would normally include slice selection gradients and an echo planar imaging readout. (b) The TDE MRI sequence considered in this paper oriented in the x-direction. This TDE sequence is identical to the Stejskal-Tanner sequence, except that a set of weak diffusion encoding gradients are added orthogonally to the direction of the primary (axial) diffusion encoding gradients. The orthogonal (radial) diffusion encoding gradients typically would have a shorter diffusion time and pulse duration than the axial gradients, so that the radial b-value is small in comparison to the axial b-value.

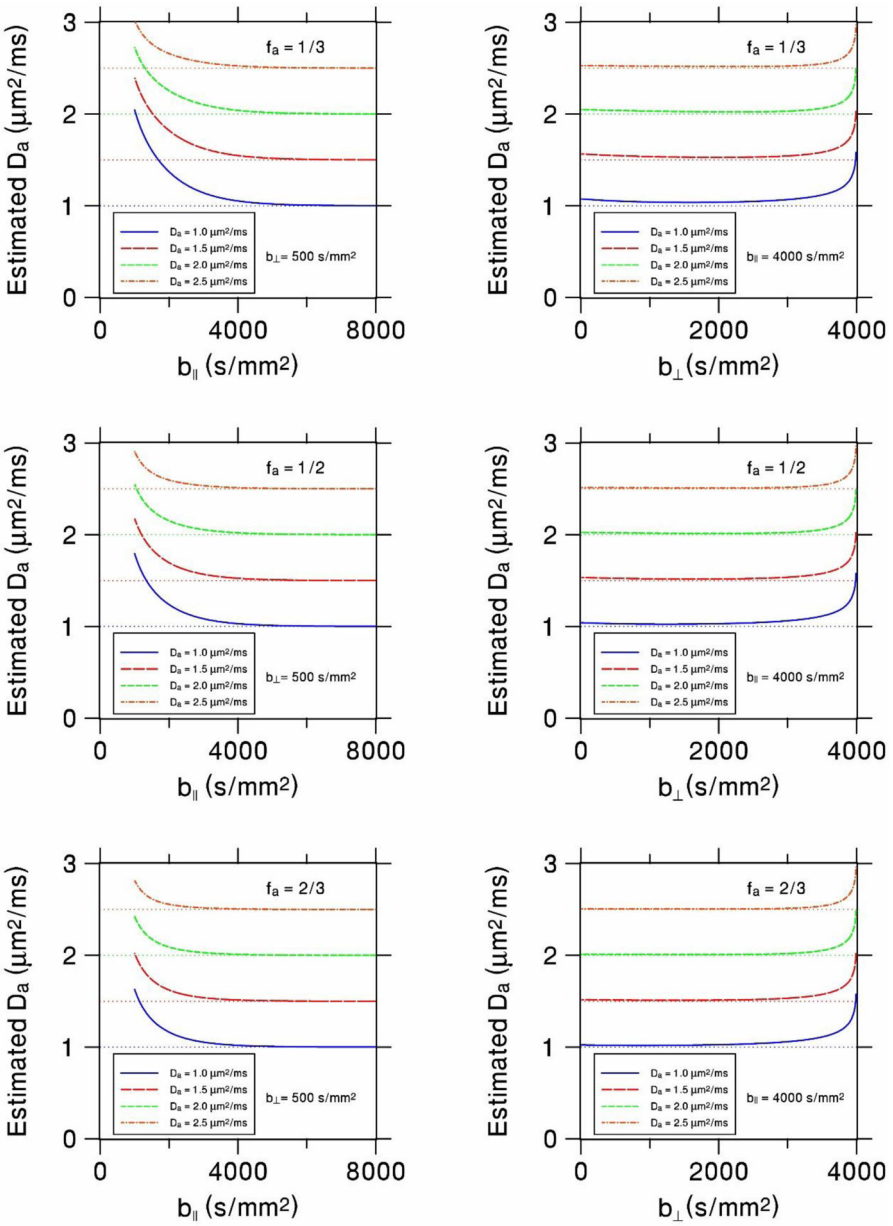

Figure 2:

Numerical simulations of the estimated intra-axonal diffusivity, D_a, as a function of the axial b-value, $b_\parallel$, (left column) and of the radial b-value, $b_\perp$, (right column). The curves show D_a as predicted by Equation 14 for a model system in which the direction-averaged extra-axonal dMRI signal is given by Equation 25, with $\lambda_{e,\parallel} = 2.0$ μm^2/ms and $\lambda_{e,\perp} = 1.0$ μm^2/ms. In the left column, the radial b-value for the TDE sequence is set to 500 s/mm^2, while in the right column the axial b-value is set to 4000 s/mm^2. For the left column, the estimated D_a is close to the exact D_a (horizontal dotted lines) for $b_\parallel > 4000$ s/mm^2. The convergence to the exact values becomes more rapid as the intra-axonal water fraction, f_a, increases, since a higher intra-axonal water fraction implies a smaller contribution to the signal from extra-axonal

water. The right column shows the estimated D_a to be largely insensitive to the choice of $b_\perp$ for $b_\perp < 2000$ s/mm^2.

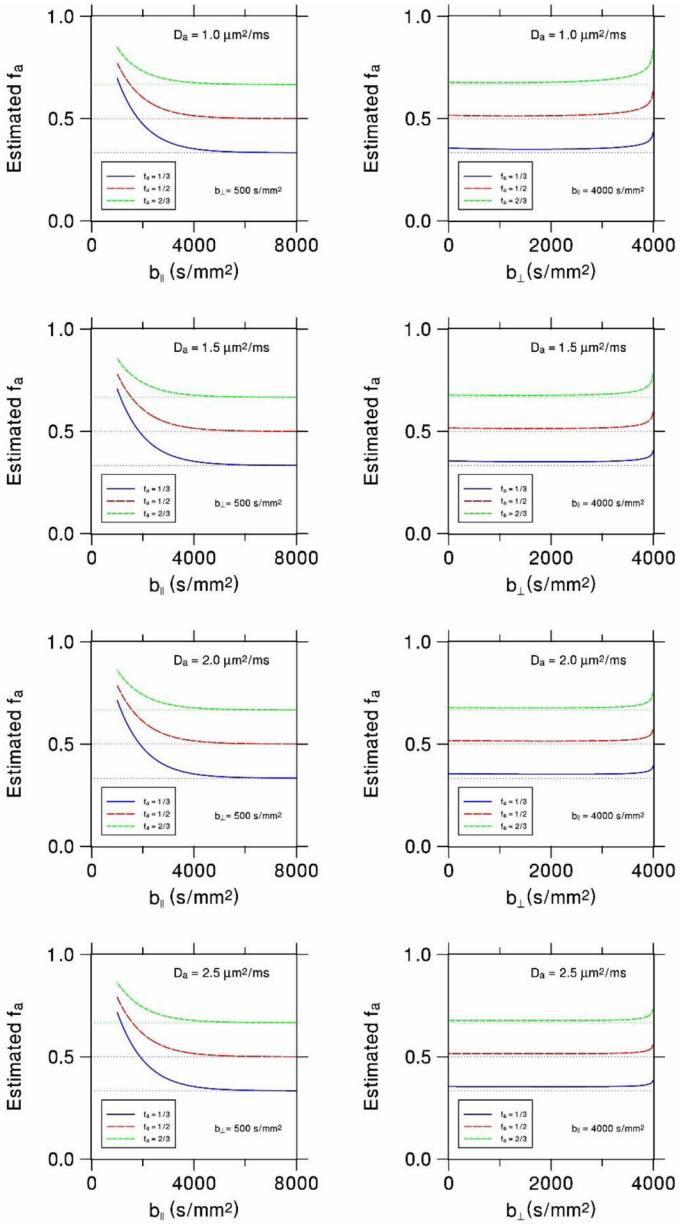

Figure 3:

Numerical simulations of the intra-axonal water fraction, f_a, as a function of the axial b-value, $b_\parallel$, (left column) and of the radial b-value, $b_\perp$, (right column). The curves show f_a as predicted by Equation 13 for the same model system and parameters as in Figure 2. Once again, the estimated values for the left column are close to the exact values (horizontal dotted lines) when $b_\parallel$ is larger than about 4000 s/mm^2, while in the right column they are seen to be insensitive to $b_\perp$ for $b_\perp$ less than about 2000 s/mm^2. The accuracy of the predicted intra-axonal water fraction varies only slightly with the D_a, for the range of values considered as long as $b_\perp < 2000$ s/mm^2.